



A Signature-Based Search for Anomalous $\ell\gamma\cancel{E}_T + \text{b-jet}$ Production and SM $t\bar{t} + \gamma$ Production in 6.0 fb^{-1} with the CDF-II detector

The CDF Collaboration
URL <http://www-cdf.fnal.gov>
(Dated: February 10, 2011)

We present a search for anomalous production of the signature $\ell + \gamma + \text{b-quark} + \cancel{E}_T$ ($\ell\gamma\cancel{E}_T b$) produced in $p\bar{p}$ collisions at $\sqrt{s} = 1.96 \text{ TeV}$ using 6.0 fb^{-1} of data taken with the CDF detector in Run II at the Tevatron. In addition to the $\ell\gamma\cancel{E}_T b$ signature-based search, we present a search for top pair production with an additional radiated photon, $t\bar{t} + \gamma$. We find 85 $\ell\gamma\cancel{E}_T b$ events versus an expectation of 99.1 ± 7.61 events. Additionally requiring the events to contain at least 3 jets and to have a total transverse energy of 200 GeV, we observe 30 $t\bar{t}\gamma$ candidate events versus an expectation from non-top standard model (SM) sources of 13.0 ± 2.1 . Assuming the difference between the observed number and the predicted non- $t\bar{t}\gamma$ SM total is due to $t\bar{t}\gamma$ production, we measure the $t\bar{t}\gamma$ cross section to be 0.18 ± 0.07 (stat.) ± 0.04 (sys.) ± 0.01 (lum.) pb. We also measure a ratio of the $t\bar{t}\gamma$ cross section to the $t\bar{t}$ cross section to be 0.024 ± 0.009 . Several control samples were constructed to validate background modelling such as dilepton+ γ ($\ell\ell\gamma$), and $l + \gamma + \cancel{E}_T$ ($\ell\gamma\cancel{E}_T$), and a pretagged $t\bar{t}$ sample.

I. INTRODUCTION

An important test of the standard model (SM) of particle physics [2] is to measure and understand the properties of the highest momentum-transfer particle collisions, and therefore to study interactions at the shortest distances. The major predictions of the SM for these collisions are the rates for the events of a given type, and their associated kinematic distributions.

However, the predicted high-energy behavior of the SM becomes unphysical at an interaction energy on the order of several TeV. Therefore, new physical phenomena are required to ameliorate this high-energy behavior. These unknown phenomena may involve new fundamental forces, new elementary particles, and/or a modification of space-time geometry. The new phenomena are likely to manifest themselves as an anomalous production rate of a combination of the known fundamental particles.

The unknown nature of possible new phenomena in the energy range accessible at the Tevatron is the motivation for a “signature-based” search strategy that does not focus on a single model or class of models of new physics, but casts a wide net for new phenomena.

In this note we present a search for anomalous production of events with a high- P_T lepton (electron, e or muon, μ), photon (γ), jet tagged as containing b-meson (b-jet), and missing transverse energy (\cancel{E}_T) ($\ell\gamma\cancel{E}_Tb$ events), using 6.0 fb^{-1} of integrated luminosity from $\bar{p}p$ collisions at $\sqrt{s} = 1.96\text{ TeV}$ collected using the CDF II detector [10]. To verify our object identification and background predictions, we consider various control samples as sanity checks of our methods and results.

The $\ell\gamma\cancel{E}_Tb$ signature is possible [4] in different models beyond the SM, such as gauge-mediated Supersymmetry (SUSY) models [5]. The signature has known SM backgrounds, and could be produced in decays of heavy particles. This type of signature contains fundamental particles, such as two third-generation quarks, t-quark and b-quark, and two gauge bosons, W ($W \rightarrow \ell\nu$) and γ . This search is related to the $\ell\gamma + X$ search [8], but with a b-tag requirement in addition to lower photon E_T ; lepton P_T and \cancel{E}_T requirements are unchanged.

One of the largest SM processes contributing to $\ell\gamma\cancel{E}_Tb$ is the $t\bar{t}\gamma$ signature. The SM $t\bar{t}\gamma$ process should have a large total transverse energy, a scalar quantity that is the sum of E_T ’s and P_T ’s of all objects in the event (leptons, photons, \cancel{E}_T , jets), and denoted as H_T . Using the $\ell\gamma\cancel{E}_Tb$ signature but requiring 3 or more jets, and large H_T greatly reduces SM processes, while retaining much of the SM $t\bar{t}\gamma$ signature. It is found that requiring a χ^2 cut on low E_T photons can remove many jets faking photons events, and negligibly reduces SM $t\bar{t}\gamma$ acceptance. A control sample of $l + \gamma + \cancel{E}_T$ ($\ell\gamma\cancel{E}_T$), and dilepton+ γ ($\ell\ell\gamma$) events (described in Sec. IV) is used to model both true photons and objects faking photons. The explanation of the χ^2 cut is in Appendix A. This search is an improvement of a previous $t\bar{t}\gamma$ analysis, described in detail in Ref. [3].

A search for the $t\bar{t}\gamma$ signature neglecting to look for the photon is a search for the production of top pairs, and is a control sample for non-photon background measurements of $t\bar{t}\gamma$. Measuring the ratio of the $t\bar{t}\gamma$ production cross section to that of $t\bar{t}$ production provides a precision measurement that is of importance for the LHC experiments.

II. DATA SAMPLE & EVENT SELECTION

This analysis is based on an integrated luminosity of 6.0 fb^{-1} collected with the CDF-II detector between March 2002 and January 2010. The data are collected with an inclusive lepton trigger that requires an electron (muon) with $E_T > 18\text{ GeV}$ ($P_T > 18\text{ GeV}$). From this inclusive lepton dataset we select events offline with two of the following: a reconstructed isolated electron E_T (muon P_T) greater than 20 GeV, missing $E_T > 20\text{ GeV}$, at least 3 jets with $E_T > 15\text{ GeV}$, a photon with E_T greater than 10 GeV, and a SecVtx [7] b-tagged jet with E_T greater than 15 GeV.

III. OVERVIEW OF THE MEASUREMENT

Each of our signatures are made up of a collection of specific objects such as muons, photons, and electrons. Before we describe our signatures we begin by describing the identification of the individual objects.

A muon candidate passing the “tight” cuts must have: a) a well-measured track in the COT; b) energy deposited in the calorimeter consistent with expectations; c) a muon “stub” in both the CMU and CMP,

or in the CMX, consistent with the extrapolated COT track; and d) COT timing consistent with a track from a $p\bar{p}$ collision. An electron candidate passing the “tight” selection must have: a) a high-quality track with $P_T > 0.5 E_T$, unless $E_T > 100$ GeV, in which case the P_T threshold is set to 20 GeV; b) a good transverse shower profile that matches the extrapolated track position; c) a lateral sharing of energy in the two calorimeter towers containing the electron shower consistent with that expected; and d) minimal leakage into the hadron calorimeter [1].

Photon candidates are required to have $E_T^\gamma > 10$ GeV, no track with $P_T > 1$ GeV, and at most one track with $P_T < 1$ GeV, pointing at the calorimeter cluster; good profiles in both transverse dimensions at shower maximum; and minimal leakage into the hadron calorimeter [1].

The measurement of the production cross sections of $t\bar{t}$ and $t\bar{t}\gamma$ is performed in a lepton plus jets channel where $t\bar{t}(t\bar{t}\gamma) \rightarrow W^+W^-b\bar{b}(\gamma)$ and one of the W bosons decays into a lepton and neutrino, and the other decays to quarks. We also perform a signature-based search in the $\ell\gamma\cancel{E}_T b$ channel looking for anomalous production not predicted by the SM.

Candidate events for the $t\bar{t}\gamma$ sample are a subset of the $\ell\gamma\cancel{E}_T b$ sample which further requires the H_T to be greater than 200 GeV, and 3 jets with E_T greater than 15 GeV. Photons in our $t\bar{t}\gamma$ sample are expected, primarily, to be isolated. Photons are copiously produced from jet decays, such as decays of η or π^0 to photons. However, photons from π^0 decays should be collimated, with little separation. These photons are likely to have a more spread out distribution in the hits in the Central Electromagnetic Shower detector (CES). This leads to a higher χ^2 value for a photon from jet decays. We use a cut on χ^2 of a photon with $10 \text{ GeV} \leq E_T \leq 25 \text{ GeV}$ in the $t\bar{t}\gamma$ sample based on the optimization in the $\ell\gamma\cancel{E}_T$ and $\ell\ell\gamma$ control samples; we explain this fully in Appendix A.

Finally, candidate events for the $t\bar{t}$ sample are chosen to be as similar to $t\bar{t}\gamma$ events as possible and require: a reconstructed isolated electron E_T (muon P_T) greater than 20 GeV, missing $E_T > 20$ GeV, at least 3 jets with $E_T > 15$ GeV and $|\eta| < 2.0$, one of which has been SecVtx b-tagged jet. The amount of QCD pollution is reduced by requiring $H_T > 200$ GeV and a transverse mass of the lepton and \cancel{E}_T to be greater than 10 GeV for muons and 20 GeV for electrons.

Background processes enter our event selection and contribute as backgrounds to the $t\bar{t}\gamma$ and $t\bar{t}$ cross-section measurements. These include W+jets, QCD, jets faking photons, and electrons faking photons, and several electroweak processes. The estimates of these background processes are derived from a combination of Monte Carlo (MC) and Data-Driven methods which are described below.

A. Monte Carlo Based Backgrounds

The rates of the backgrounds for our samples, as well as our signatures, $t\bar{t}$, $t\bar{t}\gamma$ are calculated using an MC based approach. Several electroweak processes can contribute to the $t\bar{t}\gamma$, and $\ell\gamma\cancel{E}_T b$ samples including, WW, WZ, ZZ, as well as $Wb\bar{b}\gamma$, $Wc\bar{c}\gamma$, and $Wc\gamma$ decays. For the $t\bar{t}$ sample we model with MC the backgrounds: $Wb\bar{b}$, $Wc\bar{c}$, and Wc decays, as well as diboson, and single top production.

The contribution to our sample is calculated:

$$N_{p\bar{p} \rightarrow X} = \sigma_{p\bar{p} \rightarrow X} \cdot A \times \epsilon \cdot \int dt \cdot \mathcal{L} \quad (1)$$

where $\sigma_{p\bar{p} \rightarrow X}$ is the theoretical cross section, $\int dt \cdot \mathcal{L}$ is the total integrated luminosity, and $A \times \epsilon$ is the acceptance of the signal times the selection efficiency. Many of the MC samples used were generated with 1 fb^{-1} statistics, so we must normalize these samples to our total integrated luminosity. The samples also have a scale factor ϵ which is based on object identification and trigger efficiencies which differ between data and MC. These efficiencies are averaged over all data periods and vary by lepton type.

Furthermore, for the W decay MC (W+HF, $W\gamma$ +HF) in the $t\bar{t}$ sample there are two K-factors required to account for differences between generated MC and what is observed in the detector. A k-factor is an overall scale that must be applied to the samples to augment their rate. The W+HF MC was generated with only tree-level processes, and an additional factor of 1.36 is necessary to account for the differences between leading-order processes and next-to-leading-order processes. In addition it has been found that the W+HF MC does not correctly model the heavy flavor content in the sample; it requires an additional correction of 1.5 ± 0.3 . These two factors are applied multiplicatively to the above equation.

B. Leptons from Non-W sources

The contribution to our signals due to Non-W (QCD) sources is measured using the anti-electron method [6]. An anti-electron is an object that is kinematically very similar to a real electron, however this object fails two or more quality cuts of a real electron. We use the kinematic distributions of these objects to model events with leptons due to QCD contamination of our samples.

The \cancel{E}_T distribution is used in our samples without requiring the \cancel{E}_T cut (e.g. for the $t\bar{t}$ sample, we only require a tight lepton, large H_T , 3 jets or more, with 1 b-tagged jet) for each of our samples.

In the low \cancel{E}_T region, QCD events should be substantial and there should be a deficit between the number of events observed in data, and the number of events, not due to QCD, predicted. We assume this difference is due to QCD events. In the 0-20 GeV region of \cancel{E}_T we fit a scaled distribution of \cancel{E}_T from the anti-electrons sample to the difference between data and MC samples, and for $t\bar{t}$ a mistagged sample of events. A mistagged sample of events for the $\ell\gamma\cancel{E}_T b$ and $t\bar{t}\gamma$ signatures is not used because we will be using a method of overlap removal between events due QCD and events due to jets mistagged as b-jets; we discuss this further in Sec. III F.

The anti-electron distribution has a multiplicative scale factor to minimize the χ^2 between the data and backgrounds in the 0-20 GeV region of \cancel{E}_T . Fig. 1 shows a plot of the \cancel{E}_T range for data (black), $t\bar{t}$ MC (green), and anti-electrons (red).

The entries in the scaled distribution of anti-electrons in the \cancel{E}_T signal region (above 20 GeV) is then summed over, and this is our measurement of the amount of events due to QCD processes, N_{QCD} .

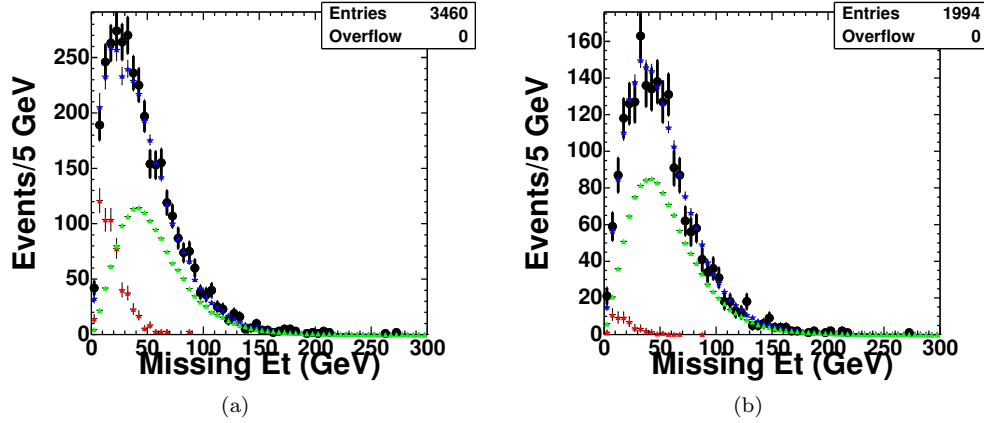


FIG. 1: Anti-electron and data distribution for the $t\bar{t}$ signature. The red points are scaled antielectrons, green points are from the $t\bar{t}$ MC, and blue is all MC, as well as the distribution of mistags and the antielectrons summed together. We see good agreement in the 0-20 GeV region which determines the scale factor of the antielectrons, and the 20- ∞ shows good agreement as well. The antielectrons' distributions show that the majority of the QCD signal is in the low \cancel{E}_T range.

C. Mistags

A secondary vertex can be identified when poorly reconstructed tracks seem to cross each other near the origin. A secondary vertex that does not originate from a heavy flavor (HF) quark decay is called a mistag.

The negative tag rate is found to be well parameterized by five jet parameters (jet E_T , number of good SVX tracks, the sum of all jet E_T in the event, jet η , and jet ϕ), and is measured in a very high statistics sample derived from triggers on high- P_T jets. This background looks at taggable jets, a jet capable of faking a b-tagged jet which has two or more good SevVtx tracks. In each of our samples, we find the probability of a taggable jet to be misidentified as having heavy-flavor.

The total number of mistagged events, N_- for a signature is:

$$N_- = \sum \left(1 - \prod_j^{N_{jets}} \bar{P}_j \right) \quad (2)$$

where \bar{P}_j is the probability that the jet in question, j , was not mistagged (the complement of the probability of a jet being mistagged). The mistag probability for the event is the complement of the event not having a mistagged event. The total number of mistagged events is summed over all events matching the criteria of a signature without requiring the b-tagged jet. The amount of mistagged events overpredicts the total number of events in the $t\bar{t}$ sample, because we are counting in N_- events from $W+HF$, $t\bar{t}$, single top, and other decays that typically have real b-meson decay. To correct this we look at the amount of events not due to these type of events in the pretagged sample, and remove from the pretagged total those events which typically would have a b-meson decay. The amount of pretagged events left over are said to be due to $W + \text{Light Flavor (LF)}$. The ratio of $W + \text{LF}$ to the total pretagged sample is used to scale the total amount of mistags, N_- . The following formula details the calculation of $W + \text{LF}$ and the total amount of mistags:

$$N_{mistags} = \frac{N_-}{N_{PT}} (N_{PT} - N_{PT}^{t\bar{t}} - N_{PT}^{QCD} - N^{W+HF} - N_{PT}^{EWK} - N_{PT}^{singletop}) \quad (3)$$

where EWK denotes those samples of Z +jets decays, and diboson decays, and the subscript PT denotes pretagged. This correction is applied in a similar way for both the $\ell\gamma E_T b$ and $t\bar{t}\gamma$ samples. However we do not remove the N_{QCD} from these samples, we remove it via a double counting prescription as described below.

D. Jets Faking Photons

High P_T photons are copiously created from hadron decays in jets initiated by a scattered quark or gluon. In particular, mesons such as the π^0 or η decay to photons which may satisfy the photon selection criteria. We measure the rate of these fakes by examining all photon candidates which pass our photon cuts, except for isolation requirements. We plot the photon candidates' calorimeter isolation, and fit the shape to the isolation of electrons from $Z^0 \rightarrow e^+e^-$ decays, and a straight line. The shape from the $Z^0 \rightarrow e^+e^-$ decays represents true photons' calorimeter isolation shape, and the straight line is a fit to the background of jets capable of faking photons. It is then straightforward to find the amount of jets faking photons by integrating the area under the straight line between 0-2 GeV in isolation; the signal region of photons. We show a plot of the photon candidates' calorimeter isolation in Fig. 2, these are from the high statistics $\ell\gamma E_T$ control sample (described in Sec. IV).

E. Electrons Faking Photons

The rate at which an electron fakes a photon is parameterized by the E_T of the electron. The probability function comes from looking for $Z^0/\gamma^* \rightarrow e\gamma$ events and $Z^0/\gamma^* \rightarrow e^+e^-$ events. One can find the rate of observing a photon based on its E_T , $N_\gamma(E_T)$, and the rate of observing an electron from a $Z^0/\gamma^* \rightarrow e^+e^-$ decay as $N_e(E_T)$. The ratio of $N_\gamma(E_T)$ to $N_e(E_T)$ gives the rate for an electron to fake a photon based for a specific E_T . A fit through several E_T points can be used as a functional form of the probability of an electron to fake a photon based on its E_T .

F. Double Counting

In order to make the background estimate as precise as possible it is necessary to compensate for the fact that some data-driven backgrounds have overlapping samples. For example, the sample of jets faking photons, and the mistagging of light-flavor jets as b-tagged jets, have a large overlap.

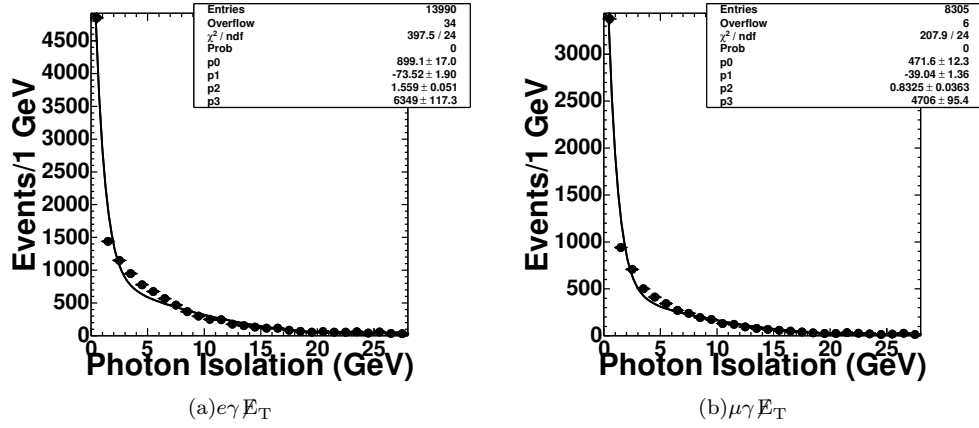


FIG. 2: Spectrum of photon candidate isolation for $e\gamma E_T$ (a) and $\mu\gamma E_T$ (b) samples. The signal region for true photons is between 0 and nearly 2 GeV. The long tail after 2 GeV is dominated by fake photons. The values p0 and p1, are the y-intercept and slope of the straight line fit, while p2, and p3 are parameters of the $Z^0 \rightarrow e^+e^-$ isolation shape

The sample for jets faking photons in the $\ell\gamma E_T b$ signature requires significant E_T , ℓ , $j \rightarrow \gamma$, and a b-tagged jet. While the sample for a mistagged light-flavor jet is E_T , ℓ , $j \rightarrow b$, and a photon. An event that has E_T , ℓ , $j \rightarrow \gamma$, $j \rightarrow b$, and a b-jet, will then be counted once in the jets faking photons sample, and once in the mistag category.

This is done for each pair of the 6 data-driven background pairs in the case of $\ell\gamma E_T b$, and $t\bar{t}\gamma$ signals. For each case the rate at which both objects could be misidentified is calculated, and half of the resulting overlap is subtracted from each of the data-driven background pairs for the final signal and background tables. The amount of double counting of events from the $\ell\gamma E_T b$ sample is shown in Table I.

CDF Run II Preliminary, 6.0fb^{-1}			
Lepton + Photon + E_T + b Events, Isolated Leptons			
Double Counting Source	$e\gamma b E_T$	$\mu\gamma b E_T$	$(e + \mu)\gamma b E_T$
Jets Faking Photons and Electrons Faking Photons	0.0085	0	0.00850
Jets Faking Photons and Mistags	3.92	1.90	5.820
Jets Faking Photons and QCD	0	0	0
Electrons Faking Photons and QCD	0	0	0
Mistags and QCD	0.18	0.0032	0.180
Mistags and electrons faking photons	0.25	0.10	0.253
Total amount of Double Counting	4.36	2.00	6.360

TABLE I: Total amount of double counting from the $\ell\gamma E_T b$ sample. We do this for both $t\bar{t}\gamma$ and $\ell\gamma E_T b$ samples.

IV. CONTROL SAMPLES

Several control samples were used to validate our data-driven backgrounds. The $\ell\gamma E_T$ sample was constructed to validate our jets faking photons, electrons faking photons, and non-W data-driven backgrounds, these are discussed in greater detail in Secs. IIID, IIIE, and IIIB respectively. We also constructed a pretagged sample of $t\bar{t}$, where we dropped our requirement for a tagged b-jet.

The $\ell\gamma E_T$ sample was chosen to be similar to the $\ell\gamma E_T b$ sample, therefore we looked for high- P_T electrons or muons, $E_T > 20$ GeV, and a photon with $E_T > 10$ GeV. This sample had 4462 $e\gamma E_T$ events,

and $3814 \mu\gamma\cancel{E}_T$ events (compared to a SM prediction of 4800 ± 500 and 3500 ± 300 respectively). This signal is dominated by $W\gamma$ events, and events where jets fake photons. Unlike the $\ell\gamma\cancel{E}_T b$ and $t\bar{t}\gamma$ samples, we are not statistics limited when we find the amount of jets faking photons in this sample, and this helps us to estimate the systematic uncertainty on the jets faking photons background measurement. Furthermore, while the electrons faking photons background is small, relative to $W\gamma$ and jets faking photons, in this sample, it is still an important part of our measurement in the $\ell\gamma\cancel{E}_T$ sample and this allows a large-scale check of our method. The QCD background measurement is a large background in the $\ell\gamma\cancel{E}_T$ sample and is estimated as mentioned above (Sec. III B), and allows us to check the systematic errors on the measurement.

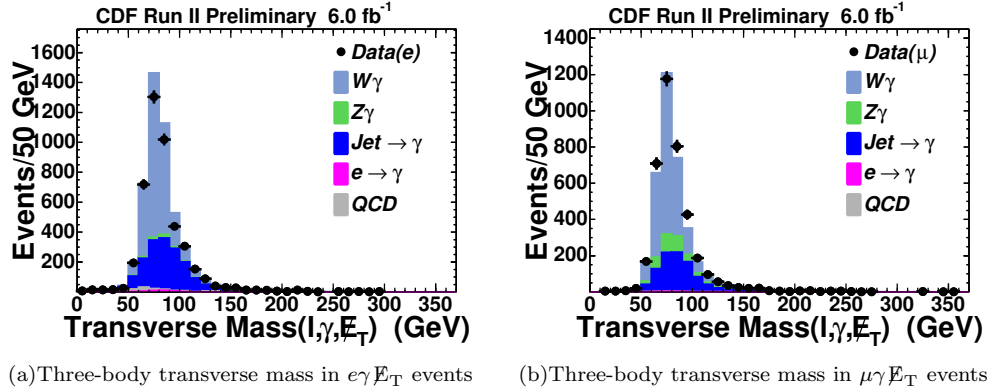


FIG. 3: Spectrum of Three-Body Transverse Mass for $\ell\gamma\cancel{E}_T$ events

The pretagged $t\bar{t}$ sample is an ideal control sample for $t\bar{t}$ because the only non-MC background is the QCD sample. This provides a great cross-check on our QCD measurement technique for $t\bar{t}$, and allows us to check on K-factors that W+HF MC samples require. We find 10968 pretagged $t\bar{t}$ events decaying to electrons and 6969 pretagged $t\bar{t}$ decaying to μ events (compared to a SM prediction of 10980 ± 2200 and 7204 ± 1440 respectively). This sample is dominated by a W+LF background. The K-factors due to Heavy Flavor content have a large uncertainty associated with them (Sec. III A), and this drives the uncertainty on the histograms as shown in Fig. 4. The generated cross section of the $t\bar{t}$ MC (6.7 pb) is used in the plots. The W+LF background samples require the same K-factor for higher order corrections, 1.36 , but require a K-factor for heavy flavor content of 1.1 ± 0.2 .

V. FULL SIGNAL AND BACKGROUND PREDICTION

The following section shows our full prediction of signal and background predictions for the $\ell\gamma\cancel{E}_T b$, $t\bar{t}\gamma$ and $t\bar{t}$ samples and the results are presented below. Table II summarizes the background and signal of the $t\bar{t}$ sample using our measured cross section for $t\bar{t}$, and we show kinematic validation plots for this signature in Fig. 5. We explain the full calculation of the cross section in Sec. VII, and Table III shows the background and signal of the $\ell\gamma\cancel{E}_T b$ sample, and Table IV summarizes the signal and background for $t\bar{t}\gamma$. In Fig. 6, and Fig. 7 we show kinematic validation plots of the $\ell\gamma\cancel{E}_T b$ and $t\bar{t}\gamma$ samples respectively.

VI. SYSTEMATIC UNCERTAINTIES

Systematic uncertainties are calculated by varying a given parameter within its uncertainty and seeing the effect on a given MC or data-driven background, and summing, in quadrature if they are independent, all such effects on the signal and backgrounds. We describe each of the systematics below.

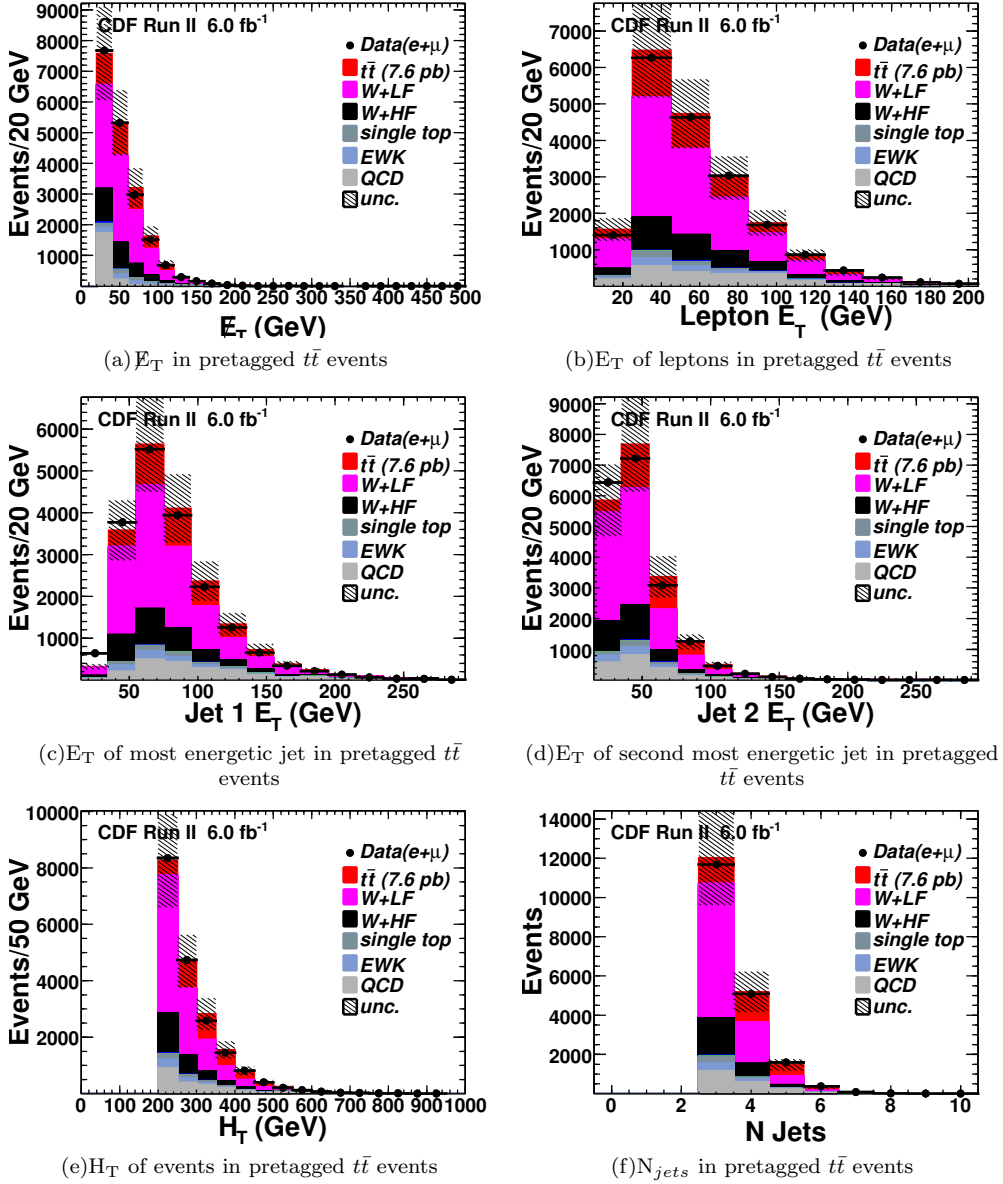


FIG. 4: Spectrum of kinematic distributions for pretagged $t\bar{t}$ events. a) the missing transverse energy; b) the transverse energy (momentum) for electrons (muons); c) the transverse momentum of the most energetic jet; d) the transverse momentum of the second most energetic jet; e) the total transverse energy (H_T) f) the number of jets in the event. The black dots are data, and the histograms are MC and data-driven backgrounds. The K-factors due to Heavy Flavor content have a large uncertainty associated with them, and this drives the uncertainty on the histograms. The generated cross section of $t\bar{t}$ (6.7 pb) is used in the plots.

A. Jet Energy Scale

To measure the effect of the jet energy uncertainties in the calorimeters we fluctuate the energy of each jet in our signal up and down one standard deviation and find the effect of this systematic on the total cross-section measurement to be about 1%.

CDF Run II Preliminary, 6.0 pb⁻¹			
<i>t\bar{t}</i> , Isolated Leptons, 3 or more jets, H _T > 200 GeV			
Standard Model Source	<i>eb</i> \cancel{E}_T	<i>μb</i> \cancel{E}_T	(<i>e</i> + <i>μ</i>) <i>b</i> \cancel{E}_T
<i>t\bar{t}</i>	1420 ± 180	1080 ± 140	2500 ± 330
<i>WW</i>	29 ± 4	22 ± 3	51 ± 7
<i>WZ</i>	8.64 ± 1.1	6.48 ± 0.9	15.12 ± 2.0
<i>ZZ</i>	1.3 ± 0.2	1.0 ± 0.1	2.3 ± 0.3
<i>W[±]b\bar{b}</i> (inclusive)	203 ± 34	146 ± 24	348 ± 58
<i>W[±]c\bar{c}</i> (inclusive)	127 ± 23	94 ± 17	221 ± 40
<i>W[±]c</i> (inclusive)	85 ± 13	61 ± 9	147 ± 23
Single top (s-channel)	76 ± 10	59 ± 8	135 ± 18
Single top (t-channel)	66 ± 9	50 ± 7	116 ± 16
<i>Z</i> → <i>ll</i> + <i>b\bar{b}</i>	31 ± 3	22 ± 2	53 ± 5
<i>Z</i> → <i>ττ</i>	6 ± 8	9 ± 8	14 ± 11
Mistags	358 ± 29	214 ± 17	572 ± 46
QCD (jets faking <i>l</i> and \cancel{E}_T)	222 ± 38	20 ± 3	240 ± 40
Total SM Prediction	2630 ± 196	1790 ± 146	4420 ± 340
Observed in Data	2720	1709	4429

TABLE II: Expected and Observed number of events with the *t \bar{t}* signature. We measure the cross section to be $7.62 \pm 0.20(\text{stat.}) \pm 0.68(\text{sys.}) \pm 0.46(\text{lum.})$ pb., and are using that value in the above table, which is in agreement with CDF combined results $\sigma_{t\bar{t}} = 7.50 \pm 0.31(\text{stat.}) \pm 0.34(\text{sys.}) \pm 0.15(\text{lum.})$ pb.

B. Tagging

The amount of SecVtx tags in Monte Carlo is not modeled properly and as a result we must scale the overall tagging rate, 0.97, by a factor with a 5% error.

C. Mistags

We use a systematic uncertainty of 8% on the total amount of predicted mistagged events as done in the previous *t \bar{t} γ* analysis [3]. We also found the uncertainties on the parameters we are using in the MistagMatrix and confirmed that this uncertainty is reasonable.

D. QCD Contamination

The systematic uncertainty associated with our method of measuring the QCD contribution to our samples is quoted as 8% [6] by the authors of the method.

E. Jets Faking Photons

The $\ell\gamma\cancel{E}_T$ control sample was assembled (Sec. IV), which has a very large jets faking photons contribution to the background, as a result it is not statically limited. We vary parameters in the fitting of the photon candidates' isolation shape and find the systematic error to be about 20%.

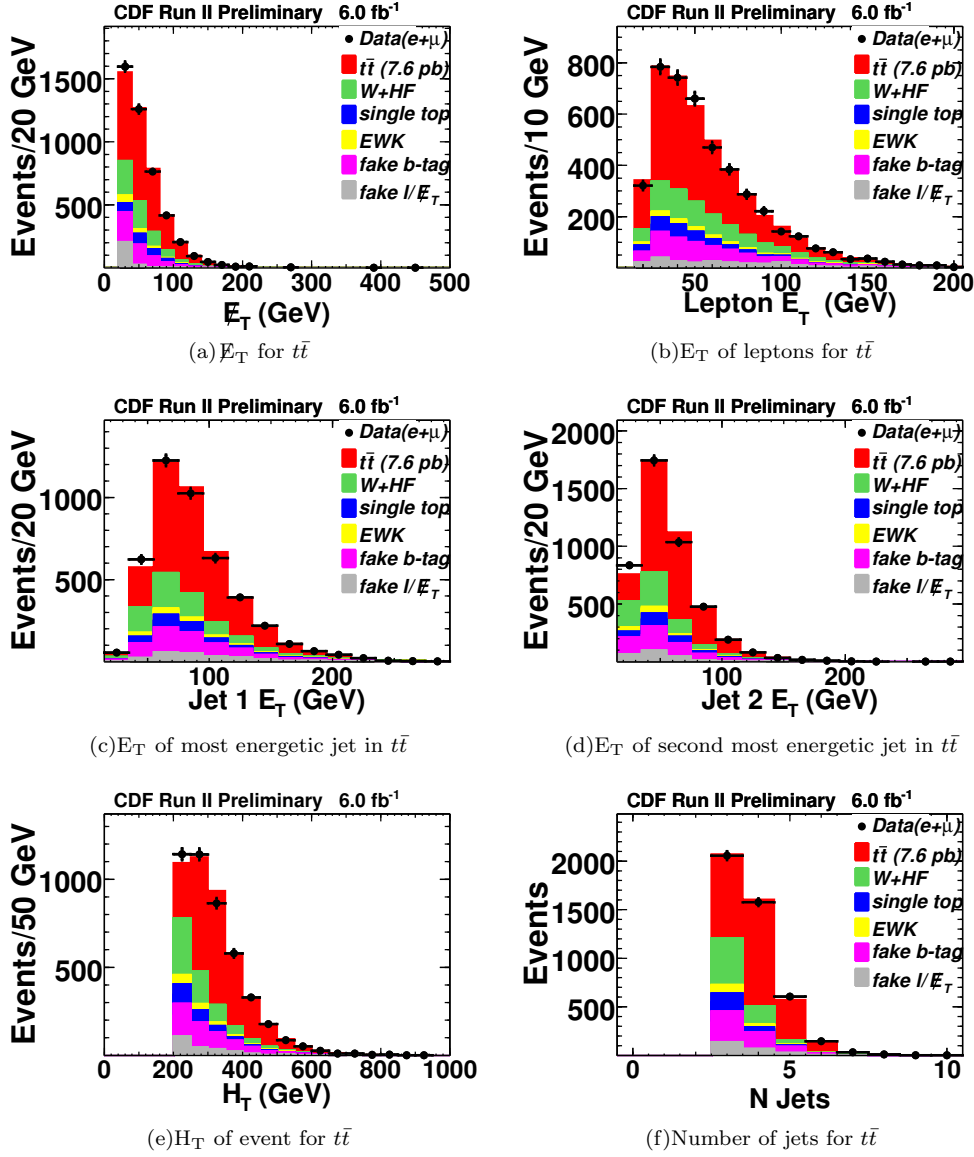


FIG. 5: Spectrum of kinematic distributions for $t\bar{t}$ events. We show in a) the missing transverse energy; b) the transverse energy (momentum) for electrons (muons); c) the transverse momentum of the most energetic jet; d) the transverse momentum of the second most energetic jet; e) the total transverse energy (H_T) f) the number of jets in the event. The black dots are data, and the histograms are MC and data-driven backgrounds.

F. Electron Faking Photons

When modeling the background due to electrons faking photons for our samples, the events are weighted by the probability of an electron to fake a photon. The probability of faking a photon depends on the electron's E_T , and some other parameters. Each parameter in probability has an associated error. To calculate the uncertainty, each of the parameters is allowed to fluctuate, and the resulting changes to the estimate are added in quadrature.

CDF Run II Preliminary, 6.0 fb⁻¹			
Lepton + Photon + \cancel{E}_T + b Events, Isolated Leptons			
Standard Model Source	$e\gamma b\cancel{E}_T$	$\mu\gamma b\cancel{E}_T$	$(e + \mu)\gamma b\cancel{E}_T$
$t\bar{t}\gamma$ semileptonic	6.74 ± 1.24	5.91 ± 1.08	12.65 ± 2.29
$t\bar{t}\gamma$ dileptonic	3.90 ± 0.71	3.39 ± 0.62	7.29 ± 1.32
$W^\pm c\gamma$	2.29 ± 0.45	2.42 ± 0.47	4.71 ± 0.73
$W^\pm c\bar{c}\gamma$	0.25 ± 0.11	0.75 ± 0.22	1.00 ± 0.24
$W^\pm b\bar{b}\gamma$	1.92 ± 0.32	1.46 ± 0.27	3.38 ± 0.48
WZ	0.23 ± 0.10	0.089 ± 0.07	0.31 ± 0.12
WW	0.29 ± 0.07	0.26 ± 0.06	0.55 ± 0.10
Single Top (s-chan)	0.54 ± 0.24	0.46 ± 0.22	1.00 ± 0.34
Single Top (t-chan)	1.13 ± 0.45	0.83 ± 0.38	1.96 ± 0.61
$\tau \rightarrow \gamma$ fake	0.37 ± 0.11	0.37 ± 0.11	0.74 ± 0.17
Jet faking γ ($ej\cancel{E}_T b, j \rightarrow \gamma$)	8.88 ± 2.57	5.28 ± 1.67	14.16 ± 3.85
Mistags	17.37 ± 1.71	12.02 ± 1.18	29.43 ± 2.75
QCD(Jets faking ℓ and \cancel{E}_T)	14.39 ± 7.33	1.44 ± 0.73	15.83 ± 7.38
$ee\cancel{E}_T b, e \rightarrow \gamma$	4.86 ± 0.71	–	4.86 ± 0.71
$\mu e\cancel{E}_T b, e \rightarrow \gamma$	–	1.32 ± 0.23	1.32 ± 0.23
Total SM Prediction	$63.2 \pm 8.1(tot)$	$36.0 \pm 2.6(tot)$	$99.1 \pm 9.3(tot)$
Observed in Data	51	34	85

TABLE III: Comparison between data and monte carlo for the $\ell\gamma\cancel{E}_T b$ sample of events. We see no significant deviations from predictions.

G. Photon Identification

The photon identification efficiency is 4% and this uncertainty is added in quadrature in the acceptance systematic uncertainty, as well as the uncertainty for MC samples with photons.

H. Trigger Efficiency

Detector specific corrections are applied to the MC to more correctly model the relative trigger efficiencies. Our lepton selection and triggering is dependent on different pieces of the CDF-II detector. These are the Central Electromagnetic (CEM), Central Muon and Central Muon Upgrade (CMUP), and Central Muon Extension (CMX) triggers.

The uncertainty due to trigger efficiency is modeled using data-derived Z events and has a small uncertainty associated with them. There are two types of corrections trigger ID and trigger efficiencies. The resulting errors are added in quadrature to the total systematic uncertainty.

I. Heavy Flavor Corrections

There is a correction factor applied to the W+HF MC to account for a mis-modelling of the amount of heavy flavor contribution found in the 1 and 2 jet bins where W+HF should dominate. This correction is applied in our signal region of 3 or more jets. The correction factor is 1.5 ± 0.3 hence the uncertainty on the correction factor is 20% on the W+HF MC.

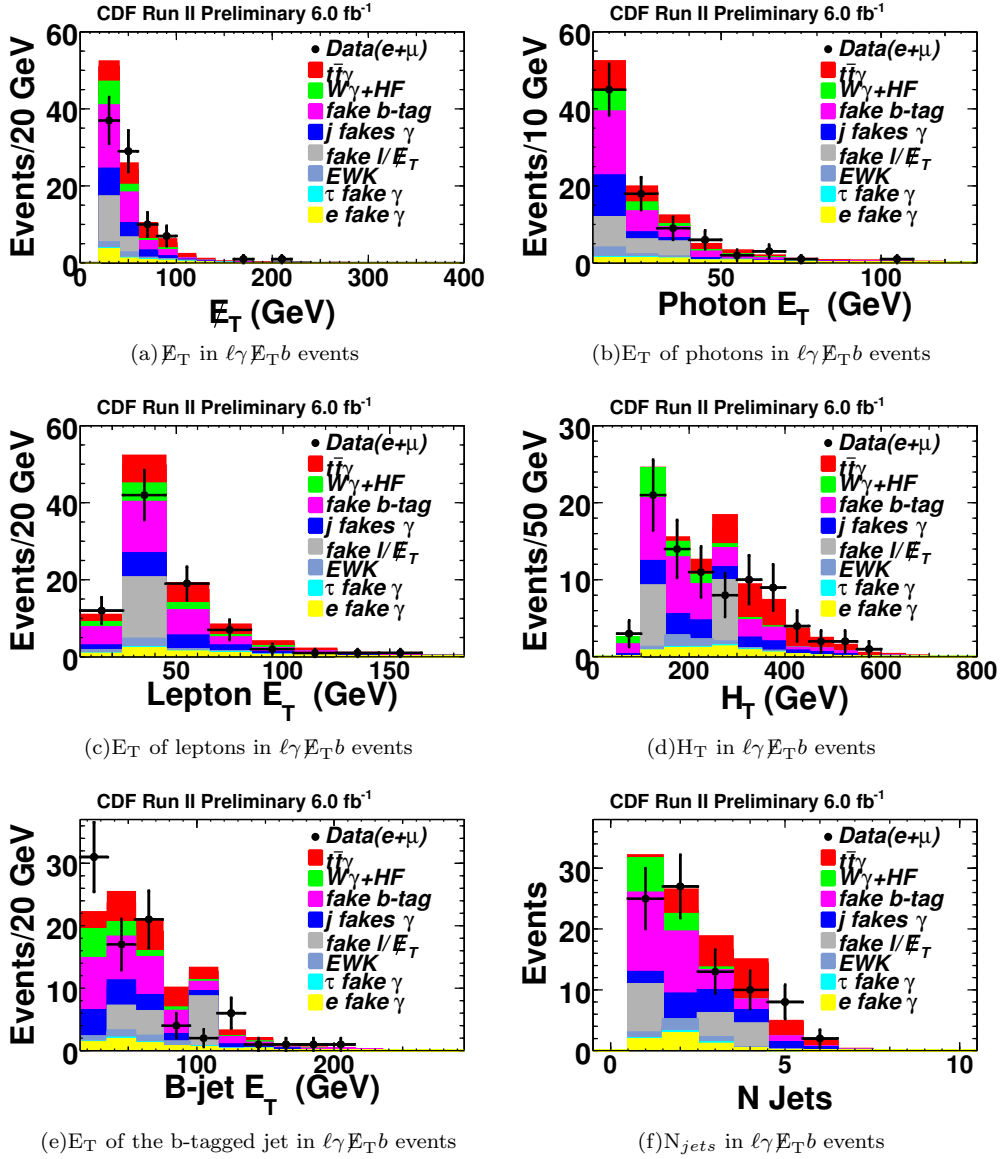


FIG. 6: Spectrum of kinematic distributions for $\ell\gamma E_T b$ events. We show in: a) the missing transverse energy; b) the transverse energy of the identified photon; c) the transverse energy (momentum) for electrons (muons); d) the total transverse energy (H_T); e) the transverse momentum of the identified b-jet; f) the number of jets in the event. The black dots are data, and the histograms are MC and data-driven backgrounds.

J. Luminosity

The uncertainty in our luminosity is derived from detector accuracy and the theoretical cross section for the inelastic $p\bar{p}$ collisions. The uncertainty on the luminosity is 6%, and we fluctuate the systematic to see its effect on our cross-section measurements. This uncertainty is for MC backgrounds.

CDF Run II Preliminary, 6.0 fb⁻¹			
<i>t\bar{t}</i> γ, Isolated Leptons, Tight Chi2 on Photons			
Standard Model Source	<i>e</i> γ <i>b</i> \cancel{E}_T	<i>μ</i> γ <i>b</i> \cancel{E}_T	(<i>e</i> + <i>μ</i>)γ <i>b</i> \cancel{E}_T
<i>t\bar{t}</i> γ(<i>semileptonic</i>)	5.98 ± 1.10	5.21 ± 0.97	11.19 ± 2.04
<i>t\bar{t}</i> γ(<i>dileptonic</i>)	1.47 ± 0.27	1.27 ± 0.24	2.74 ± 0.50
<i>W</i> [±] <i>c</i> γ	0 ± 0.07	0 ± 0.07	0 ± 0.09
<i>W</i> [±] <i>c</i> \bar{c} γ	0 ± 0.05	0.05 ± 0.05	0.05 ± 0.07
<i>W</i> [±] <i>b</i> \bar{b} γ	0.15 ± 0.07	0.06 ± 0.05	0.21 ± 0.08
<i>WZ</i>	0.05 ± 0.05	0.05 ± 0.05	0.09 ± 0.06
<i>WW</i>	0.06 ± 0.03	0.06 ± 0.03	0.11 ± 0.03
Single Top (s-chan)	0.09 ± 0.10	0 ± 0.10	0.09 ± 0.13
Single Top (t-chan)	0.14 ± 0.14	0.13 ± 0.14	0.27 ± 0.19
τ → γ fake	0.20 ± 0.08	0.10 ± 0.05	0.29 ± 0.09
Jet faking γ (<i>ej</i> \cancel{E}_T <i>b</i> , <i>j</i> → γ)	5.75 ± 1.76	1.79 ± 1.56	7.54 ± 2.53
Mistags	1.47 ± 0.37	1.02 ± 0.32	2.50 ± 0.51
QCD(Jets faking <i>ℓ</i> and \cancel{E}_T)	0.38 ± 0.38	0.02 ± 0.020	0.40 ± 0.38
<i>ee</i> \cancel{E}_T <i>b</i> , <i>e</i> → γ	0.94 ± 0.19	–	0.94 ± 0.19
<i>μe</i> \cancel{E}_T <i>b</i> , <i>e</i> → γ	–	0.49 ± 0.11	0.49 ± 0.11
Total SM Prediction	16.7 ± 2.2(<i>tot</i>)	10.3 ± 1.9(<i>tot</i>)	26.9 ± 3.4(<i>tot</i>)
Observed in Data	17	13	30

TABLE IV: Comparison between data and MC for the *t \bar{t}* γ sample of events. Here we have applied a χ^2 cut of 6 for Photons with E_T less than 25 GeV, based on the optimization studies performed on *Z*γ and discussed in Sec. A. We see good agreement between predictions and data.

VII. CROSS SECTION CALCULATIONS

The theoretical production cross section of *t \bar{t}* at the Tevatron is found to be $7.08^{+0.00+0.36}_{-0.32-0.27}$ [20]. The first uncertainty is from scale variation by a factor of 2 around $\mu = m_t$, and the second is from pdf uncertainties. A SM estimate for the leptonic cross section of *t \bar{t}* γ $\sigma_{semileptonic t\bar{t}\gamma} = 0.0943 \text{ pb} * 0.977 = 0.092 \text{ pb}$. We use a LO generator (MadGraph) to find the leptonic cross section of *t \bar{t}* γ to be 0.0943 pb, and multiply this by a $k_{factor} = \sigma_{NLO}/\sigma_{LO} = 0.977$ [21]. We then find the total production cross section by dividing by the branching ratio of *t \bar{t}* → leptons 0.543. The production cross section of *t \bar{t}* γ is the predicted to be $\sigma_{t\bar{t}\gamma} = 0.17 \pm 0.02 \text{ pb}$ Using these theoretical cross sections we compute the ratio of $\sigma_{t\bar{t}\gamma}$ to $\sigma_{t\bar{t}}$ to be $0.024^{+0.012}_{-0.014}$.

The cross section of *t \bar{t}* , $\sigma_{t\bar{t}}$ is calculated in the usual way as

$$\sigma_{t\bar{t}} = \frac{N_{obs} - N_{bckg}}{A_{t\bar{t}} \times \int \mathcal{L} dt} \quad (4)$$

where N_{obs} is the number of events with our event selection for *t \bar{t}* .

For the *t \bar{t}* sample equation 4 becomes:

$$\sigma_{t\bar{t}} = \frac{(4429 \pm 66.55) - (1916.16 \pm 28.58 \pm 96.26)}{6.0\text{fb}^{-1}(0.05497 \pm 0.00456)} \quad (5)$$

For *t \bar{t}* events in 3 or more jets, we find a cross section of

$$7.62 \pm 0.20(\text{stat.}) \pm 0.68(\text{sys.}) \pm 0.46(\text{lum.}) \text{ pb.}$$

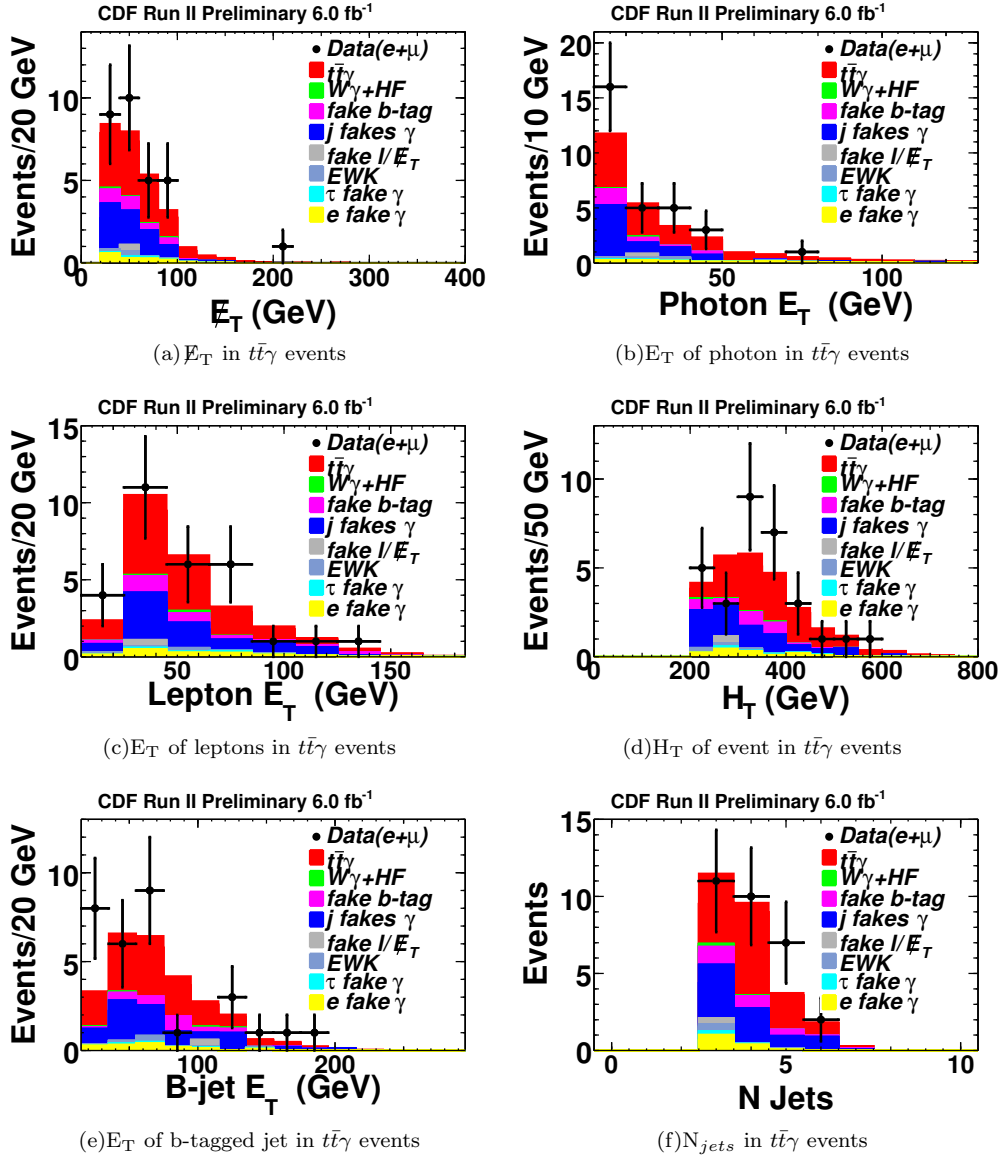


FIG. 7: Spectrum of kinematic distributions for $t\bar{t}\gamma$ events. We show in: a) the missing transverse energy; b) the transverse energy of the identified photon; c) the transverse energy (momentum) for electrons (muons); d) the total transverse energy (H_T); e) the transverse momentum of the identified b-jet; f) the number of jets in the event. The black dots are data, and the histograms are MC and data-driven backgrounds.

For the $t\bar{t}\gamma$ semileptonic cross-section measurement equation 4 becomes:

$$\sigma_{t\bar{t}\gamma} = \frac{(30 \pm 5.47) - (13.0 \pm 2.11 \pm 2.6)}{6.0\text{fb}^{-1}(0.0286 \pm 0.00378)} \quad (6)$$

We find the semi-leptonic $t\bar{t}\gamma$ cross section to be:

$$0.10 \pm 0.03(\text{stat}) \pm 0.02(\text{sys.}) \pm 0.01 (\text{lum.}) \text{ pb.}$$

and then find the total $t\bar{t}\gamma$ cross section to be:

$$0.18 \pm 0.07(\text{stat}) \pm 0.04(\text{sys.}) \pm 0.01 (\text{lum.}) \text{ pb.}$$

The probability of the backgrounds alone (i.e. if $t\bar{t}\gamma$ is not permitted in the SM) yielding 30 or more events is 0.0015, or 3.0σ .

Finally we compute the ratio between the production cross sections of $t\bar{t}\gamma$ and $t\bar{t}$ to be:

$$\mathcal{R} = 0.024 \pm 0.009 \text{ (stat.)} \pm 0.001 \text{ (sys.)}.$$

All of our cross-section measurements agree well with theoretical predictions as well as previous similar measurements. The measurement on the ratio of production cross sections of $t\bar{t}\gamma$ and $t\bar{t}$ is the first measurement of this type, and agrees well with a theoretical prediction.

Acknowledgments

We thank the Fermilab staff and the technical staffs of the participating institutions for their vital contributions. We thank Uli Baur for invaluable help with our analysis and help for generating MC processes, and help finding theoretical predictions of both the $t\bar{t}$ and the $t\bar{t}\gamma$ cross sections for the Tevatron. Tim Steltzer, Steve Mrenna, and Fabio Maltoni, Soushi Tsuno, were very helpful for their support and development for MadGraph and Pythia and help with our MC. This work was supported by the U.S. Department of Energy and National Science Foundation; the Italian Istituto Nazionale di Fisica Nucleare; the Ministry of Education, Culture, Sports, Science and Technology of Japan; the Natural Sciences and Engineering Research Council of Canada; the National Science Council of the Republic of China; the Swiss National Science Foundation; the A.P. Sloan Foundation; the Bundesministerium fuer Bildung und Forschung, Germany; the Korean Science and Engineering Foundation and the Korean Research Foundation; the Particle Physics and Astronomy Research Council and the Royal Society, UK; the Russian Foundation for Basic Research; the Comision Interministerial de Ciencia y Tecnologia, Spain; and in part by the European Community's Human Potential Programme under contract HPRN-CT-20002, Probe for New Physics.

APPENDIX A: JUSTIFICATION OF χ^2 CUT ON LOW E_T PHOTONS

In order to obtain a cut on a photon's χ^2 value, we constructed an $\ell\gamma E_T$ sample. We isolated a sample of very pure photons with E_T between 10 and 25 GeV from $Z\gamma \rightarrow \ell\ell\gamma$ decays where the three body mass of the $\ell\ell\gamma$ was between 86 and 96 GeV (Fig. 8(b)). A sample of fake photons was found by reversing the calorimeter isolation cut for photons with E_T between 10 and 25 GeV in the $\ell\gamma E_T$ decays. For χ^2 values in steps of 2, from 2 to 20, we checked to see what fraction of photons from our $Z\gamma$ sample survived and called this value our purity. The ratio of pure photons to pure and fake photons in the $\ell\gamma E_T$ sample (with photon E_T between 10 and 25 GeV) was the efficiency of the cut. A good compromise between efficiency and purity was reached at a χ^2 value of 6, this can be seen in Fig. 8(a).

-
- [1] The fraction of electromagnetic energy allowed to leak into the hadron compartment $E_{\text{had}}/E_{\text{em}}$ must be less than $0.055 + 0.00045 \times E_{\text{em}}(\text{GeV})$ for central electrons, less than 0.05 for electrons in the end-plug calorimeters, less than $\max[0.125, 0.055 + 0.00045 \times E_{\text{em}}(\text{GeV})]$ for photons.
 - [2] S.L. Glashow, Nucl. Phys. **22** 588, (1961); S. Weinberg, Phys. Rev. Lett. **19** 1264, (1967); A. Salam, Proc. 8th Nobel Symposium, Stockholm, (1979).
 - [3] T. Aaltonen *et al*, Searching the inclusive $\ell\gamma E_T$ + b-quark for radiative top quark decay and non-standard-model processes, Phys. Rev. D **80**, 011102(R), (2009);
 - [4] Baur, U., Juste, A., Orr, L. H. and Rainwater, D., Probing electroweak top quark couplings at hadron colliders, Phys. Rev. D, **71**, 054013 (2005)
 - [5] S. Ambrosanio, G.L. Kane, G.D. Kribs, S.P. Martin, and S. Mrenna, Phys. Rev. D **55**, 1372 (1997); B.C. Allanach, S. Lola, K. Sridhar, Phys. Rev. Lett. **89**, 011801 (2002); hep-ph/0111014
 - [6] B. Cooper, A. Messina (CDF Collaboration) Estimation of the background of $W \rightarrow e^\pm \nu + n$ Jet Events, /CDF/PHYS/JET/PUBLIC/7760 (2005)
 - [7] B. Acosta et.al. (CDF Collaboration) Measurement of the $t\bar{t}$ production cross section in $p\bar{p}$ collisions at $\sqrt{s}=1.96$ TeV using lepton + jets events with secondary vertex b -tagging, Phys. Rev. D **71** 052003 (2005)

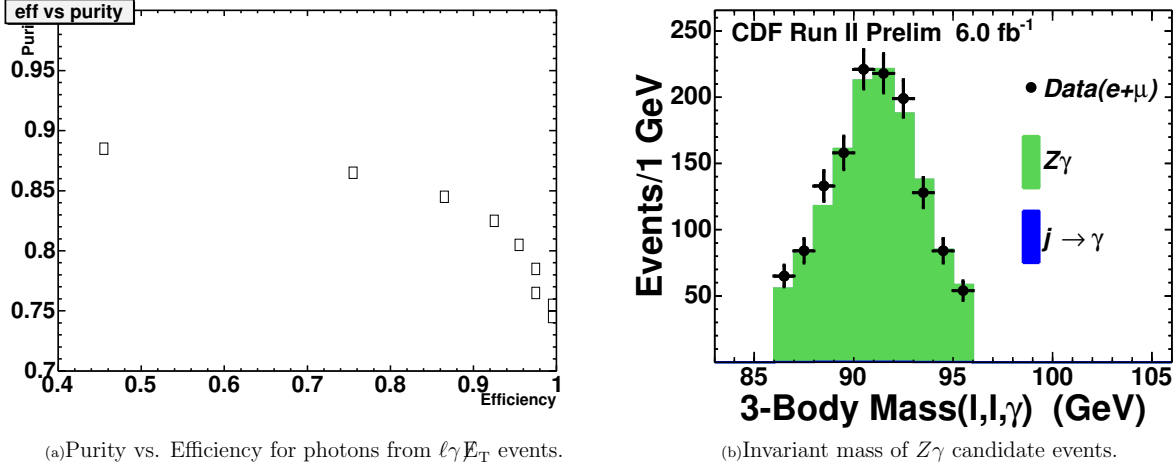


FIG. 8: Distribution of Efficiency vs Purity of Photons. True photons were collected from a $Z\gamma$ decays (3 body mass nearly the Z -mass), and fake photons had isolation > 2 . For each proposed χ^2 cut, we found the fraction of true photons and fake photons contained in a $W\gamma$ decay. The χ^2 cut goes up in steps of two from left to right and top to bottom.

- [8] A. Abulencia et al., Search for new physic in lepton+photon +X events with 929 pb $^{-1}$ of $p\bar{p}$ collisions at $\sqrt{s} = 1.96$ TeV, Phys. Rev. D **75** 112001 (2007)
- [9] M. Cacciari, et al., The $t\bar{t}$ Cross-section at 1.8 TeV and 1.96 TeV: A Study of the Systematics due to Parton Densities and Scale Dependence, JHEP **404**, 68 (2004).
- [10] D. Acosta *et al.* (CDF Collaboration), Phys. Rev. D **71**, 032001 (2005).
- [11] F. Abe, et al., Nucl. Instrum. Methods Phys. Res. A **271**, 387 (1988); D. Amidei, et al., Nucl. Instrum. Methods Phys. Res. A **350**, 73 (1994); F. Abe, et al., Phys. Rev. D **52**, 4784 (1995); P. Azzi, et al., Nucl. Instrum. Methods Phys. Res. A **360**, 137 (1995); The CDFII Detector Technical Design Report, Fermilab-Pub-96/390-E
- [12] A. Affolder *et al.*, Nucl. Instrum. Methods A **526**, 249 (2004).
- [13] A. Sill *et al.*, Nucl. Instrum. Methods A **447**, 1 (2000); A. Affolder *et al.*, Nucl. Instrum. Methods A **453**, 84 (2000); C.S. Hill, Nucl. Instrum. Methods A **530**, 1 (2000).
- [14] The CDF coordinate system of r , φ , and z is cylindrical, with the z -axis along the proton beam. The pseudorapidity is $\eta = -\ln(\tan(\theta/2))$.
- [15] S. Kuhlmann *et al.*, Nucl. Instrum. Methods A **518**, 39, 2004.
- [16] The CMU system consists of gas proportional chambers in the region $|\eta| < 0.6$; the CMP system consists of chambers after an additional meter of steel, also for $|\eta| < 0.6$. The CMX chambers cover $0.6 < |\eta| < 1.0$.
- [17] Transverse momentum and energy are defined as $P_T = p \sin \theta$ and $E_T = E \sin \theta$, respectively. Missing E_T ($\vec{\cancel{E}}_T$) is defined by $\vec{\cancel{E}}_T = -\sum_i E_T^i \hat{n}_i$, where i is the calorimeter tower number for $|\eta| < 3.6$ (see Ref. [14]), and \hat{n}_i is a unit vector perpendicular to the beam axis and pointing at the i^{th} tower. We correct $\vec{\cancel{E}}_T$ for jets and muons. We define the magnitude $\cancel{E}_T = |\vec{\cancel{E}}_T|$. We use the convention that “momentum” refers to pc and “mass” to mc^2 .
- [18] T. Sjostrand et al., High-Energy-Physics Event Generation with PYTHIA 6.1, Comput. Phys. Commun. **135**, 238 (2001).
- [19] G. Corcella et al., HERWIG 6: An Event Generator for Hadron Emission Reactions with Interfering Gluons (including supersymmetric processes), JHEP **01**, 10 (2001).
- [20] N. Kidonakis. Top quark pair and single top production at Tevatron and LHC energies, arXiv:1008.2460v1 [hep-ph] 14 Aug 2010.
- [21] D. Peng-Fei et al. QCD corrections to associated production of $t\bar{t}\gamma$ at hadron colliders, arXiv:0907.1324v2 [hep-ph] 18 Jul 2009.